



HAL
open science

Dynamic basins of attraction in a toy-model of reed musical instruments

Soizic Terrien, Baptiste Bergeot, Christophe Vergez

► **To cite this version:**

Soizic Terrien, Baptiste Bergeot, Christophe Vergez. Dynamic basins of attraction in a toy-model of reed musical instruments. Forum Acusticum, Sep 2023, Turin, Italy. hal-04294799

HAL Id: hal-04294799

<https://hal.science/hal-04294799v1>

Submitted on 20 Nov 2023

HAL is a multi-disciplinary open access archive for the deposit and dissemination of scientific research documents, whether they are published or not. The documents may come from teaching and research institutions in France or abroad, or from public or private research centers.

L'archive ouverte pluridisciplinaire **HAL**, est destinée au dépôt et à la diffusion de documents scientifiques de niveau recherche, publiés ou non, émanant des établissements d'enseignement et de recherche français ou étrangers, des laboratoires publics ou privés.



Distributed under a Creative Commons Attribution 4.0 International License

DYNAMIC BASINS OF ATTRACTION IN A TOY-MODEL OF REED MUSICAL INSTRUMENTS

Soizic Terrien^{1*}

Baptiste Bergeot²

Christophe Vergez³

¹ Laboratoire d'Acoustique de l'Université du Mans (LAUM), UMR 6613, Institut d'Acoustique - Graduate School (IA-GS), CNRS, Le Mans Université, Le Mans, France

² INSA CVL, Univ. Orléans, Univ. Tours, LaMé EA 7494,

F-41034, 3 Rue de la Chocolaterie, CS 23410, 41034 Blois Cedex, France

³ Aix Marseille Univ, CNRS, Centrale Marseille, LMA UMR7031, Marseille, France

ABSTRACT

Reed musical instruments are known to produce a wealth of sound regimes. In physical models, this complexity manifests itself by the coexistence of equilibrium, periodic and quasiperiodic regimes. From a musical perspective, controlling which regime is observed in practice when different stable regimes coexist for the same parameters can be particularly challenging. We consider a physical model of reed instrument, written as a low-order nonlinear dynamical system. A bifurcation analysis is performed to identify the multistable regions of the parameter space, where several stable regimes coexist. In these regions, the basins of attraction are investigated by means of support vector machine. The basin of a given regime corresponds to the set of initial conditions for which this regime is observed after any transient dynamics has died out, and relates to the fact that this regime is easily played in practice or not. We investigate how basins structure evolves when the mouth pressure dynamics (corresponding to attack transients) is taken into account, and highlight significant differences between the classical static basins (determined for constant values of the mouth pressure) and what we introduce as dynamical basins. In particular, some regimes are much easier to observe than predicted by the static case.

*Corresponding author: soizic.terrien@univ-lemans.fr

Copyright: ©2023 First author et al. This is an open-access article distributed under the terms of the Creative Commons Attribution 3.0 Unported License, which permits unrestricted use, distribution, and reproduction in any medium, provided the original author and source are credited.

Keywords: *musical acoustics, physical modelling, nonlinear dynamics, basins of attraction, support vector machine*

1. INTRODUCTION

Self-sustained musical instruments such as reed instruments, flutes, brass and bowed string instruments, are complex dynamical systems that can produce a wide diversity of sound regimes, whose acoustical and dynamical properties depend, often in a sensitive manner, on both geometrical parameters fixed by the instrument maker and control parameters which are adjusted continuously by the musician.

The dynamics of self-sustained instruments in general, and of reed instruments in particular, has been extensively studied in the literature [1]. Experimentally, artificial mouths allow to characterise the instrument in a reproducible manner by controlling and/or fixing the musician parameters [2, 3]. In physical models, the introduction of numerical continuation methods has lead to a much more comprehensive knowledge of the dynamics than with classical time-domain simulations. In particular, these methods give access to bifurcation diagrams representing the evolution of the different coexisting equilibrium (non-oscillating) and periodic solutions with respect to a parameter of interest. Both stable and unstable solutions are computed and bifurcation points, which correspond to qualitative changes in the system dynamics as a parameter is changed (for example, the emergence or disappearance of a periodic solutions), are also highlighted [4].

These experimental and numerical methods provide

an overall knowledge of the dynamics. In particular, different studies highlighted that the coexistence of several stable regimes for the same parameters, referred to as multistability, is very commonly observed [5]. In practice, this means that different sound regimes can be played for the exact same parameters (for example, for the same value of the mouth pressure). This raises the question of the control: how to produce reliably a particular sound regime among the different possible ones?

From the dynamical system point of view, this relates to the question of the basins of attraction. Indeed, which regime is observed in practice when a system is multistable depends on the considered initial conditions (on the state variables). The basin of attraction of a particular stable solution is defined as the set of initial conditions for which the system converges toward this particular solution after any transient dynamics has died out. A basin of attraction thus forms a subset of the phase space (i.e. the space of state variables).

In physical models of wind musical instruments, state variables are classically the modal pressures and their derivatives. It is likely that the musician do not control directly the initial conditions on these variables. On the other hand, the dynamics (i.e. time variation) of the blowing pressure has been shown to affect significantly the dynamics of the instrument, both in a physical model of reed instrument and in an actual experiment. This includes the mouth pressure thresholds at which transitions between different regimes are observed [3, 6].

We consider here the case of reed instruments, and investigate in a simple model whether the musician can use the blowing pressure dynamics to *navigate* between the different basins of attraction, and as such, to access the desired sound regime.

2. BACKGROUND ON THE PHYSICAL MODEL

2.1 Model equations

In reed musical instruments, sound production results from the nonlinear coupling between an exciter and a resonator. The exciter is constituted of an oscillating piece of wood (the reed) that acts as a valve and modulates the air flow entering the instrument. The acoustical resonator is constituted by the air column contained in the pipe of the instrument. The state-of-the-art model of reed instruments includes three main elements. First, a single degree-of-freedom oscillator equation to model the motion the reed. Secondly, a nonlinear function that links the flow entering

the instrument to the blowing pressure. Importantly, this depends on the opening of the reed channel as given by the first equation. Finally, an equation describing, in the frequency domain, the acoustical response of the resonator.

We seek here the simplest model displaying multistability on a range of control parameters. Following [1], the reed is considered through its sole stiffness (i.e. its dynamics is neglected). The reed equation thus reduces to:

$$K_r(h(t) - h_0) = p(t) - p_m, \quad (1)$$

where $h(t)$ and h_0 are the height of the reed channel and its value at rest, respectively, K_r is the equivalent stiffness of the reed, p_m is the blowing pressure and $p(t)$ is the (acoustical) pressure in the instrument mouthpiece.

The flow entering the instrument through the reed channel is given by the Bernoulli law. Physically, the reed motion amplitude is limited as it can come in contact with the instrument mouthpiece: when h is 0, the reed channel is closed. Following the so-called ghost reed model [7], this is taken into account by bringing the flow to zero when $h \leq 0$. Overall, the flow $u(t)$ entering the instrument is written as follows:

$$u(t) = \text{sign}(p_m - p(t))Wh(t)\sqrt{2\frac{|p_m - p(t)|}{\rho}}H(h), \quad (2)$$

with W the width of the reed channel, ρ the air density and H the Heaviside step function.

The response of the resonator is described in the frequency domain through its input impedance $Z_{in}(\omega)$, written as a (truncated) sum of n resonance modes:

$$Z(\omega) = \frac{P(\omega)}{U(\omega)} = Z_c \sum_{i=1}^n \frac{Z_i j\omega}{\omega_i^2 - \omega^2 + j\omega \frac{\omega_i}{Q_i}}, \quad (3)$$

with Z_i , ω_i and Q_i the modal amplitude, resonance pulsation and quality factor, respectively, of the i^{th} mode. Because we seek here the minimal model displaying multistability, we take into account a single resonance mode, with $Z_1 = 50$, $\omega_1 = 1440$ and $Q_1 = 36.6$ [8].

The model is written in dimensionless form by defining the rescaled pressure $\tilde{p}(t) = p(t)/P_M$, flow $\tilde{u}(t) = Z_c/P_M u(t)$ and time $\tilde{t} = \omega_1 t$. Here, $P_M = K_r h_0$ is the minimal blowing pressure for which the reed channel closes. Additionally, one defines the dimensionless blowing pressure $\gamma = p_m/P_M$ and dimensionless reed opening at rest $\zeta = Z_c W h_0 \sqrt{2/(\rho P_M)}$. Overall, the model can be written as a system of two first-order ordinary differential equations for the pressure in the mouthpiece $\tilde{p}(\tilde{t})$ and

its time derivative $\dot{w}(\tilde{t})$:

$$\begin{aligned}\dot{\tilde{p}}(\tilde{t}) &= \tilde{w}(\tilde{t}) \\ \dot{\tilde{w}}(\tilde{t}) &= \frac{Z_1}{Q_1} \dot{\tilde{u}}(\tilde{t}) - \frac{1}{Q_1} \tilde{w}(\tilde{t}) - \tilde{p}(\tilde{t})\end{aligned}\quad (4)$$

with:

$$\tilde{u}(\tilde{t}) = \text{sign}(\gamma - \tilde{p}(\tilde{t})) (1 - \gamma + \tilde{p}(\tilde{t})) \zeta \sqrt{|\gamma - \tilde{p}(\tilde{t})|} H(h)$$

2.2 Bifurcation diagram

A bifurcation analysis is performed using AUTO [9], a software for numerical continuation. The results, summarised in Figure 1, illustrate the behaviour of the instrument with respect to γ .

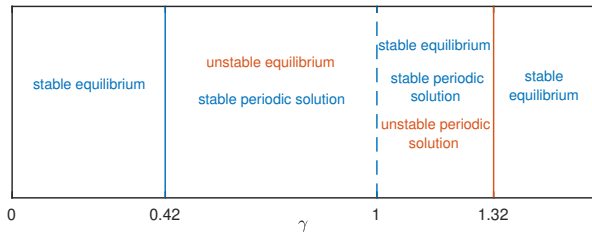


Figure 1. Results of the bifurcation analysis of (4), showing the existence and stability ranges of the different solutions with respect to γ . Vertical plain (dashed) lines indicate supercritical (subcritical) Hopf bifurcations. The red vertical line indicates a saddle-node bifurcation of periodic solutions.

For $\gamma < 0.42$, an equilibrium (non-oscillating) regime, for which no sound is produced, is the only solution. At $\gamma = 0.42$, the equilibrium solution destabilises in a supercritical Hopf bifurcation, and a stable periodic regime emerges. Increasing γ further, a subcritical Hopf bifurcation is found at $\gamma = 1$, where the equilibrium solution stabilises back and an unstable periodic solution emerges. Finally, the stable and the unstable periodic solutions collide and disappear in a saddle-node bifurcation of periodic orbits at $\gamma = 1.32$. For $\gamma > 1.32$ the only solution is the stable equilibrium. Overall, this bifurcation analysis shows that, for $\gamma \in [1; 1.32]$, the system is bistable: in this parameter region, a stable equilibrium (where no sound is produced) coexist with a stable periodic solution corresponding to a musical note.

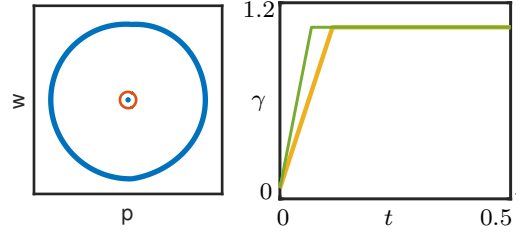


Figure 2. Left: Phase portrait of (4) for $\gamma = 1.05$ in the phase plane (\tilde{p}, \tilde{w}) . Blue (red) closed lines show a stable (unstable) periodic solution, and the blue dot represents a stable equilibrium. Right: Saturating linear ramps of γ for $\gamma(0) = 0.05$, $\gamma_t = 1.05$ and two different slopes.

2.3 Static basins of attraction

In this region of bistability, which regime is observed in practice depends on the initial conditions considered for the two state variables \tilde{p} and \tilde{w} . Because we consider here a very simple system with only two dimensions (two state variables), the boundary between the two basins of attraction is trivial, and is constituted by the unstable periodic solution that emerges from the subcritical Hopf bifurcation (see Figure 1). This is illustrated in Figure 2 (left) which shows the phase portrait of system (4) for a fixed value $\gamma = 1.05$. Depending whether the initial conditions $\tilde{p}(0)$ and $w(0)$ are chosen inside or outside the unstable periodic solution (red closed loop), the system converges towards the stable equilibrium (blue dot) or toward the stable periodic solution (blue closed loop), respectively.

3. DYNAMIC BASINS OF ATTRACTION

Focusing on the bistable region of the bifurcation diagram, we investigate whether a time variation of γ can affect the (trivial) basins of attraction. In particular, we aim at investigating if, starting from given initial conditions $\tilde{p}(0)$ and $\tilde{w}(0)$, the musician can access a different regime than predicted by the static basin of attraction by modifying only the attack transient on γ .

We consider saturating linear ramps of the dimensionless blowing pressure γ as a prototypical profile of γ during an attack transient:

$$\begin{aligned}\gamma(\tilde{t}) &= \gamma_0 + s\tilde{t} & \text{for } \tilde{t} < \tilde{t}_s, \\ \gamma(\tilde{t}) &= \gamma_t & \text{for } \tilde{t} \geq \tilde{t}_s,\end{aligned}\quad (5)$$

where γ_0 and γ_t are the initial and target values of γ , s is the slope, and $t_s = \frac{\gamma_t - \gamma_0}{s}$ is the time at which γ saturates.

Throughout this article, the saturating (target) value γ_t is fixed and is chosen in the range of bistability highlighted above. The influence of both γ_0 and s on the regime observed in the long term is investigated numerically with time-domain simulations of (4). Figure 2 (right) shows two examples of saturating linear ramps of γ , for $\gamma_0 = 0$, $\gamma_t = 1.05$ and two different values of s .

For a target value $\gamma_t = 1.05$ and a slope $s = 0.006$, Figure 3 shows the so-called *dynamic basin of attraction*. This shows, in the space of initial conditions $\tilde{p}(0)$, $\tilde{w}(0)$ and initial value γ_0 , which regime is obtained once γ_t has been reached and after any transient dynamics has died out. Blue and green zones correspond to the sets of initial conditions for which the equilibrium and periodic regime are obtained, respectively. The red closed curve indicates the boundary between the static basins of attraction for $\gamma = 1.05$, as shown in Figure 2.

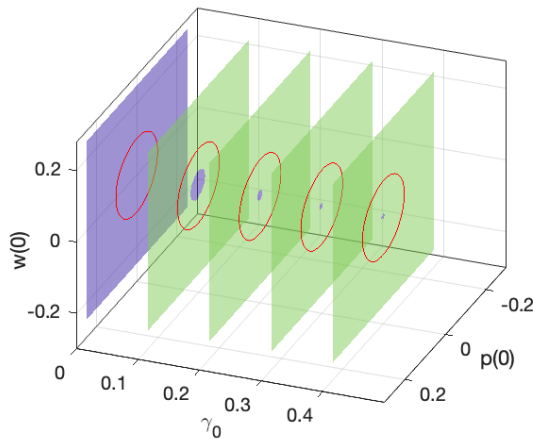


Figure 3. Dynamic basin of attraction, in the space of initial conditions on γ , \tilde{p} and \tilde{w} , for a target value $\gamma_t = 1.05$ and a slope $s = 0.006$. The regime towards which the system converges is indicated by the color code (blue for the equilibrium, green for the periodic regime). The red circle is the boundary between the corresponding *static* basin for $\gamma = \gamma_t$.

These results demonstrate that the dynamics of γ (and, as such, the attack transient produced by the musician), can significantly affect the basins of attraction

and, as such, the produced sound. In particular, the *dynamic* basin of attraction significantly differs from the *static* basin obtained for $\gamma_t = 1.05$. As figure 3 shows, it becomes impossible in practice to access the periodic regime for $\gamma_0 = 0$, as any initial condition on \tilde{p} and \tilde{w} lead to the non-oscillating regime. On the other hand, for all the other values of γ_0 considered in Figure 3, the basin of the equilibrium solution is significantly smaller than in the static case. This means that for $\gamma(0) \in [0.1; 0.4]$, it is easier to access the periodic regime (*i.e.* to produce a sound) in the dynamic case than in the static case.

3.1 A more systematic approach using a Support Vector Machine classifier

A systematic investigation of the geometry of the dynamic basins of attraction in the 3D space of initial conditions $\tilde{p}(0)$ and $\tilde{w}(0)$ and initial value of γ , for different target values γ_t and slope s , would be particularly time-consuming. Indeed, determining the dynamical basins for one set of fixed values of γ_t and s implies to perform a simulation for each set of initial conditions in the 3D space shown in Figure 3.

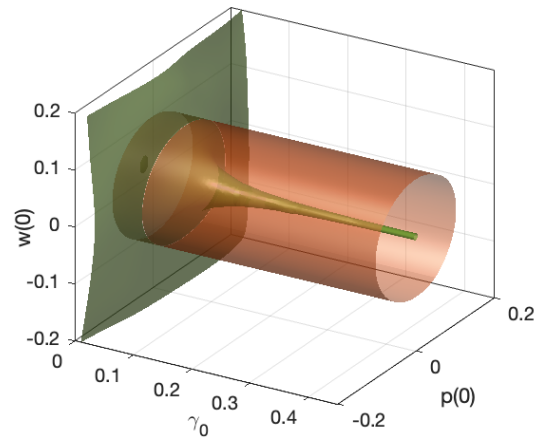


Figure 4. Boundary between the dynamic basin of attraction (green) computed with a SVM classifier for the same parameters as in Figure 3. The orange surface shows the boundary between the corresponding static basins for a fixed value $\gamma = \gamma_t$.

An alternative approach is to determine the boundaries between the basins of attraction associated to each

possible regime, in the 3D space of initial conditions on \bar{p} and \bar{w} and initial value of γ . This can be done using an Explicit Design Space Decomposition (EDSD) technique [10, 11], based on support vector machine classifiers (SVMs) [12, 13]. SVM is a machine learning technique which has been widely used for classification tasks. In musical acoustics, this has been used to determine the parameters leading to quasiperiodic oscillations (corresponding to *multiphonic* sounds) in a minimal model of single reed instruments [7]. This allows for a more systematic investigation of the dynamic basins of attraction, and of the influence of the features of the attack transient on γ , including different shapes of its time evolution.

Figure 4 shows the boundary between basins of attraction for the same parameters as in Figure 3. This demonstrates the feasibility of the method. Additionally, the computation time is considerably reduced compared to the case of a regular mesh of the 3D space. These results pave the way towards a more systematic investigation of dynamic basins of attraction with respect to the control parameters of the musician.

4. CONCLUSION

We demonstrate, in a toy model of single reed instrument, that the dynamics of the blowing pressure can significantly affect the basins of attraction, that is to say the set of initial conditions leading to a given regime when several coexist. Because this directly relates to the attack transient performed by the musician and to the *playability* of the different regimes, this is of particular interest. Our results show that for some profiles of γ , a periodic regime (corresponding to a musical note) can become more easily accessible than when a fixed, constant value of the blowing pressure is considered. The use of a Support Vector Machine classifier - a machine learning technique - will allow, in future work, a more systematic investigation of the so-called *dynamic basins of attraction*.

5. REFERENCES

- [1] A. Chaigne and J. Kergomard, *Acoustics of Musical Instruments*. Modern Acoustics and Signal Processing, Springer-Verlag New York, 2016.
- [2] D. Ferrand and C. Vergez, "Blowing machine for wind musical instrument: toward a real-time control of the blowing pressure," in *2008 16th mediterranean conference on control and automation*, pp. 1562–1567, IEEE, 2008.
- [3] B. Bergeot, A. Almeida, C. Vergez, B. Gazengel, and D. Ferrand, "Response of an artificially blown clarinet to different blowing pressure profiles," *J. Acoust. Soc. Am.*, vol. 135, no. 1, pp. 479–490, 2014.
- [4] S. Karkar, C. Vergez, and B. Cochelin, "Oscillation threshold of a clarinet model: A numerical continuation approach," *The Journal of the Acoustical Society of America*, vol. 131, no. 1, pp. 698–707, 2012.
- [5] T. Colinot, C. Vergez, P. Guillemain, and J.-B. Doc, "Multistability of saxophone oscillation regimes and its influence on sound production," *Acta Acustica*, vol. 5, p. 33, 2021.
- [6] B. Bergeot and C. Vergez, "Analytical prediction of delayed hopf bifurcations in a simplified stochastic model of reed musical instruments," *Accepted in Non-linear Dynamics*, vol. 107, pp. 3291–3312, 2022.
- [7] J.-B. Doc, C. Vergez, and S. Missoum, "A minimal model of a single-reed instrument producing quasiperiodic sounds," *Acta Acustica united with Acustica*, vol. 100, no. 3, pp. 543–554, 2014.
- [8] J. Gilbert, S. Maugeais, and C. Vergez, "Minimal blowing pressure allowing periodic oscillations in a simplified reed musical instrument model: Bouassebenade prescription assessed through numerical continuation," *Acta Acustica*, vol. 4, no. 6, p. 27, 2020.
- [9] E. J. Doedel, A. R. Champneys, F. Dercole, T. F. Fairgrieve, Y. A. Kuznetsov, B. Oldeman, R. Paffenroth, B. Sandstede, X. Wang, and C. Zhang, "Auto-07p: Continuation and bifurcation software for ordinary differential equations," 2007.
- [10] A. Basudhar and S. Missoum, "A sampling-based approach for probabilistic design with random fields," *Computer Methods in Applied Mechanics and Engineering*, vol. 198, no. 47-48, pp. 3647–3655, 2009.
- [11] A. Basudhar and S. Missoum, "An improved adaptive sampling scheme for the construction of explicit boundaries," *Structural and Multidisciplinary Optimization*, vol. 42, pp. 517–529, 2010.
- [12] N. Cristianini and B. Scholkopf, "Support vector machines and kernel methods: the new generation of learning machines," *Ai Magazine*, vol. 23, no. 3, pp. 31–31, 2002.
- [13] S. R. Gunn *et al.*, "Support vector machines for classification and regression," *ISIS technical report*, vol. 14, no. 1, pp. 5–16, 1998.